



# Journal of Applied Sciences

ISSN 1812-5654

**science**  
alert

**ANSI***net*  
an open access publisher  
<http://ansinet.com>

## Effect of Loading on the Physicochemical Properties of Alumina Supported Co/Mo Bimetallic Nanocatalysts

<sup>1</sup>Sardar Ali, <sup>2</sup>Noor Asmawati Mohd Zabidi and <sup>1</sup>Duvvuri Subbarao

<sup>1</sup>Department of Chemical Engineering, Universiti Teknologi PETRONAS,  
Sri Iskandar, Tronoh 31750, Perak, Malaysia

<sup>2</sup>Department of Fundamental and Applied Sciences, Universiti Teknologi PETRONAS,  
Sri Iskandar, Tronoh 31750, Perak, Malaysia

**Abstract:** The present research deals with the synthesis of cobalt bimetallic Co/Mo nanocatalysts supported on alumina. The nanocatalysts were prepared by wet impregnation method. The samples were characterized in terms of reducibility, dispersion and particle size using Temperature Programmed Reduction (TPR), Transmission Electron Microscopy (TEM) and BET-surface area analysis. H<sub>2</sub>-TPR analysis of Co/Al<sub>2</sub>O<sub>3</sub> indicated three temperature regions at 380°C (low temperature), 680°C (medium temperature) and 900°C (high temperature). The incorporation of molybdenum into cobalt nanocatalysts shifted the reduction temperatures towards higher temperature but the percentage of species being reduced at low temperature increased also incorporation of molybdenum reduce the crystallinity but decreased the metal particle size of the catalysts. Increasing metal loading from 5 to 10 %wt increased the reducibility of bimetallic nanocatalysts.

**Key words:** Bimetallic nanoparticles, Fischer-Tropsch synthesis, cobalt, molybdenum

### INTRODUCTION

Fischer-Tropsch (FT) synthesis is a process which deals with the conversion of syngas derived from coal, biomass and natural gas into diesel fuels consisting of paraffins, olefins, alcohols and aldehydes with a high cetane number and is environmentally friendly (Dry, 1999). As a matter of fact, due to limited petroleum reserves and environmental restrictions, FT-synthesis is gaining more attention nowadays. The FT-synthesis is considered as a surface-catalyzed polymerization reaction. During this process, CO is adsorbed on transition metal surface and hydrogenated producing CH<sub>x</sub> monomers which consequently propagate to produce products consisting of hydrocarbons and oxygenates with a broad range of functionalities and chain lengths (Brady and Pettit, 1980).

All the group VIII elements show considerable activity for this process. Among them Co, Fe and Ru displayed the highest activity (Tavasoli *et al.*, 2005). Due to their high activity for FT-synthesis, high selectivity to linear products, more stability towards deactivation, low activity towards water-gas shift (WGS) reaction and low cost compared to Ru based catalysts, cobalt based catalysts are the preferred choice for FT-synthesis (Iglesia, 1997; Jacobs *et al.*, 2002).

In many heterogeneous reactions the active phase are dispersed on a support which not only act as a carrier

but may also contribute to the catalytic activity. Al<sub>2</sub>O<sub>3</sub>, SiO<sub>2</sub> and TiO<sub>2</sub> are the commonly used supports for cobalt-based catalysts (Sundaramurthy *et al.*, 2008; Jacobs *et al.*, 2004).

The incorporation of a second metal component to the catalysts may result in the geometric or electronic modification of the catalysts which may result in the modification of adsorption characteristics of the catalysts. Cooper and co-workers (Cooper *et al.*, 2007) have used bimetallic Co-Mo for the FT-reaction. They found that incorporation of molybdenum to cobalt catalysts increases the acid-site strength causing them to be selective to lower hydrocarbons compared to mono-metallic cobalt catalysts.

This study deals with the synthesis and characterization of cobalt and molybdenum mono- and bimetallic nano-catalysts supported on  $\gamma$ -alumina. Effect of incorporation of molybdenum to cobalt catalysts and metal loading in terms of reducibility, dispersion, crystallinity and particle size distribution are presented.

### MATERIALS AND METHODS

**Catalysts synthesis:** All the monometallic and bimetallic nano-catalysts were prepared using the wet impregnation method with 5 and 10 wt.% loading. These catalysts are assigned as M%/Alumina (where M represents metal

impregnated). Before impregnation alumina (Merck, BET  $190 \text{ m}^2\text{g}^{-1}$ ) was calcined at  $500^\circ\text{C}$  for 6 h. For each catalyst, required amounts of the precursor salts i.e.,  $\text{Co}(\text{NO}_3)_2 \cdot 6\text{H}_2\text{O}$  ( $\geq 98\%$ , Fluka) and  $(\text{NH}_4)_6\text{Mo}_7\text{O}_{24} \cdot 4\text{H}_2\text{O}$  (99-101%, Fischer-Scientific) were dissolved in deionized water and added to the support dropwise with constant stirring followed by drying in an oven at  $120^\circ\text{C}$  overnight and calcining at  $500^\circ\text{C}$  for 6 h with the temperature ramping of  $5^\circ\text{C min}^{-1}$ .

**Catalyst characterization:** The reduction behaviour of the catalysts was studied using TPDRO1100 MS equipped with thermal conductivity detector. 0.5 g catalyst was placed in the U-shaped quartz tube. The catalyst samples were degassed in a flow of nitrogen at  $200^\circ\text{C}$  to remove traces of water and cooled down to room temperature. TPR was performed using 5%  $\text{H}_2/\text{N}_2$  with a flow rate of  $20 \text{ cm}^3\text{min}^{-1}$  and heating from 40 to  $900^\circ\text{C}$  at  $10^\circ\text{C min}^{-1}$ . Morphology of the catalyst samples was characterized using transmission electron microscopy (Philip Tecnai 20, accelerating voltage: 200 kv). Samples were prepared in ultrasonic dispersion of n-hexane and the suspensions were dropped onto a copper grid. The surface area, pore volume and average pore size distribution of the catalyst samples were measured using  $\text{N}_2$ -adsorption (Micromeritics, ASAP 1000).

## RESULTS AND DISCUSSION

**$\text{H}_2$ -Temperature Programmed Reduction (TPR) profiles:** The reducibility of the calcined catalysts was studied by  $\text{H}_2$ -Temperature Programmed Reduction (TPR). It is a very useful tool which reveals the reduction behavior of different oxidized phases of the catalysts. In some cases it also gives useful information about the metal particle size, metal dispersion and metal to support interaction.

As shown in Fig. 1, three peaks were observed in case of 5%  $\text{Co}/\text{Al}_2\text{O}_3$ . The peak appearing at  $381^\circ\text{C}$  was due to the reduction of  $\text{Co}_3\text{O}_4$  to  $\text{CoO}$ . The second peak appearing at  $710^\circ\text{C}$  can be attributed to the reduction of  $\text{CoO}$  to  $\text{Co}^0$  (Berge *et al.*, 2000). While the peak present at high temperature is usually attributed to the reduction of very small particles and the reduction of metal and support mixed oxides. As shown in Fig. 1, the catalyst 5%  $\text{Mo}/\text{Al}_2\text{O}_3$  showed typical reduction pattern for Mo species. The larger peak at  $467^\circ\text{C}$  can be attributed to reduction of  $\text{Mo}^{6+}$  to  $\text{Mo}^{4+}$  while the one at  $638^\circ\text{C}$  was due to the reduction of  $\text{Mo}^{4+}$  to lower species (Khodakov *et al.*, 2007). The peak appearing at higher temperature may be due to the reduction of smaller particles and mixed oxides of metal and support.

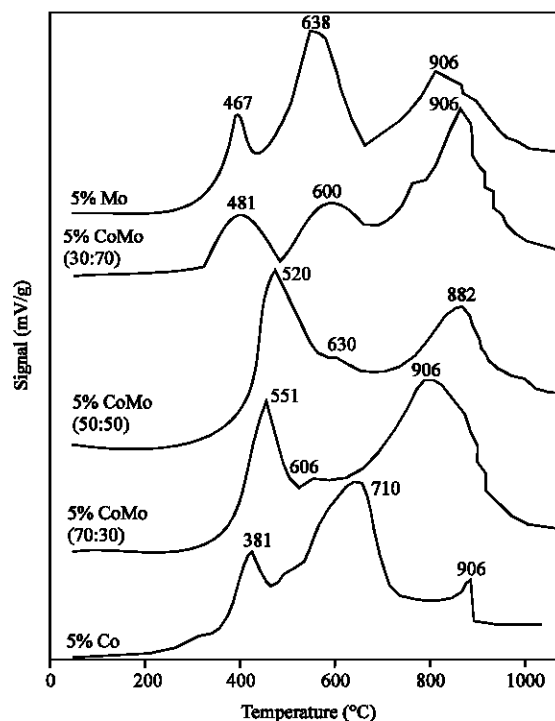


Fig. 1: TPR profiles of the catalysts

As shown in Fig. 1, for the 5%  $\text{CoMo} (70:30)/\text{Al}_2\text{O}_3$  catalyst when molybdenum was incorporated to cobalt catalysts a significantly different reduction behavior was displayed. This was different from either of the monometallic nano-catalysts. The first reduction peak shifted to  $520^\circ\text{C}$  (increased by 36%) while the second reduction peak appeared at  $630^\circ\text{C}$  (decreased by 11%). The peaks appearing at 520 and  $630^\circ\text{C}$  can be attributed to the reduction of bimetallic  $\text{CoMoO}_4$  and  $\text{MoAlO}_4$  (Chen and Adesina, 1994; Rodriguez *et al.*, 1999; Chen and Liu, 1991). With further increase in the amount of Mo incorporated for the catalyst 5%  $\text{CoMo} (70:30)/\text{Al}_2\text{O}_3$ , first reduction peak is increased by 44.6% ( $551^\circ\text{C}$ ) while the second reduction peak decreased by 14.6% ( $606^\circ\text{C}$ ) but greater percentage of the species were reduced at  $551^\circ\text{C}$ . When the Mo content was more increased for the catalyst 5%  $\text{CoMo} (30:70)/\text{Al}_2\text{O}_3$ , though the reduction occurred at lower temperature (first and second peaks appeared at 481 and  $606^\circ\text{C}$ , respectively) as shown in the Fig. 1, but majority of the species were reduced at higher temperature. Interaction of Mo to Co catalysts shifted the reduction temperatures slightly to higher temperatures and reduced the degree of dispersion but percentage of the species reduced at relatively low temperatures increased. This effect was more pronounced for the catalyst 5%  $\text{CoMo} (50:50)/\text{Al}_2\text{O}_3$ , in case of

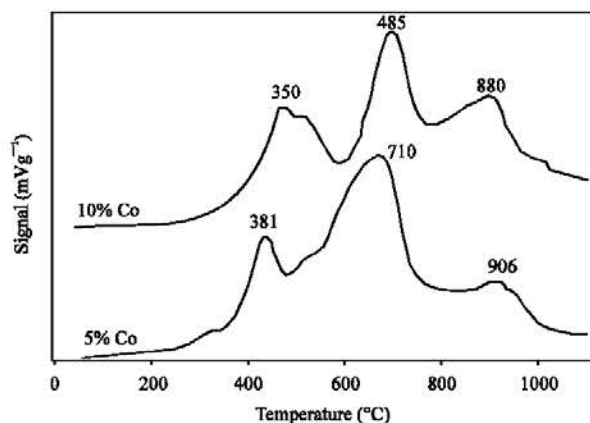


Fig. 2: TPR profiles of 5% Co/Alumina

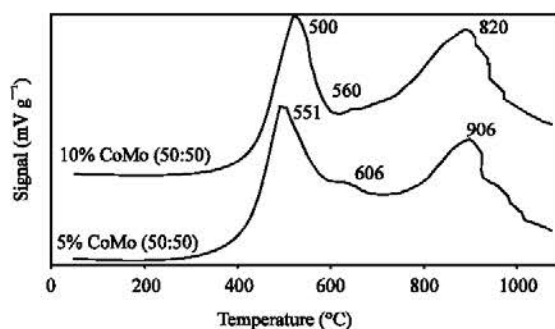


Fig. 3: TPR profiles of 5% CoMo (50:50)/Alumina and 10% CoMo (50:50)/Alumina

5 wt.% Co/Al<sub>2</sub>O<sub>3</sub> only 34% of the chemisorbed hydrogen was consumed at 350°C but with incorporation of Molybdenum, 60% of chemisorbed hydrogen was consumed in the region from 551 to 606°C.

Increase in loading from 5 to 10 wt.% enhanced the reduction which could be attributed to the increase in metal particle size with increase in metal loading as evident from the TEM images. As shown in the Fig. 2, for the catalyst 10% Co/Al<sub>2</sub>O<sub>3</sub> increase loading from 5 to 10 wt.% all the three reduction peaks shifted to lower reduction temperatures. Reduction peaks appeared at 350, 485 and 880°C which are reduced by 8.13, 31.69 and 3% respectively. This behavior was pronounced for the bimetallic nano-catalysts also. For the catalyst 10% CoMo (50:50)/Al<sub>2</sub>O<sub>3</sub>, as shown in the Fig. 3, reduction occurred at 500, 560 and 820°C, respectively much lower than 5% CoMo(50:50)/Al<sub>2</sub>O<sub>3</sub> catalyst.

**Transmission Electron Microscopy (TEM):** Figure 4 shows the Transmission Electron Microscopy (TEM) images for the 5 wt.% Co(I)/Al<sub>2</sub>O<sub>3</sub> catalyst. Average particle size of the catalysts was calculated from the TEM images are summarized in Fig. 5 and 6.

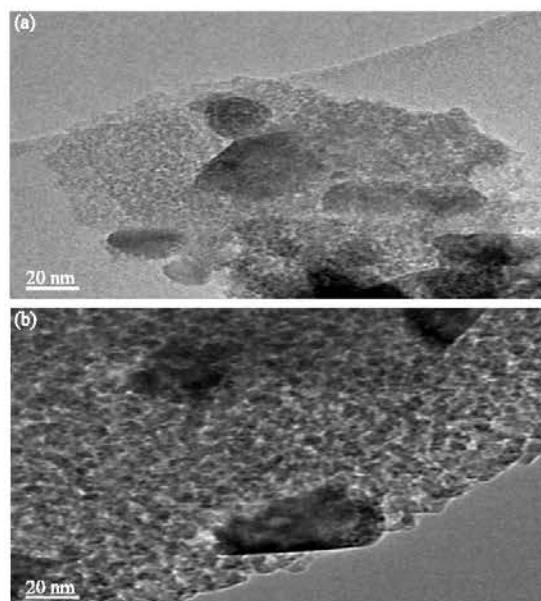


Fig. 4: TEM images of the catalysts. (a) 5% Co/Alumina and (b) 5% CoMo (50:50)/Alumina

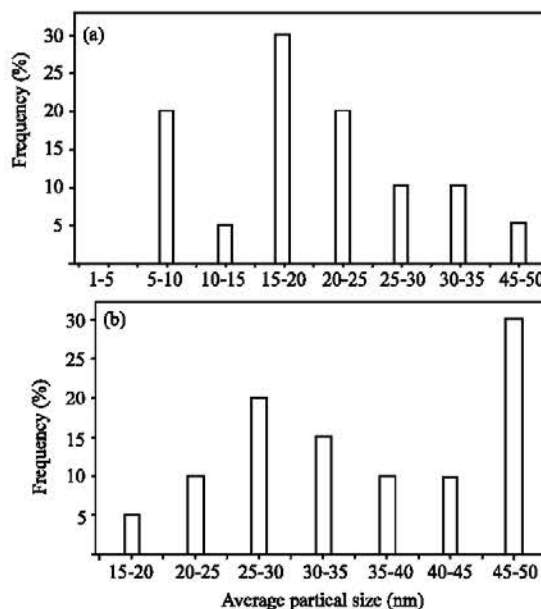


Fig. 5: TEM plots of the catalysts; (a) 5% and (b) 10% Co/Alumina

For 5 wt.% Co/Al<sub>2</sub>O<sub>3</sub> shown in Fig. 5 (a), 30% of the particles were in size range from 15-20 nm. The increase in loading from 5 to 10 wt.% resulted in increase in metal particle size. For 10 wt.% Co/Al<sub>2</sub>O<sub>3</sub> the metal particle size ranged from 45-50 nm (Fig. 5b).

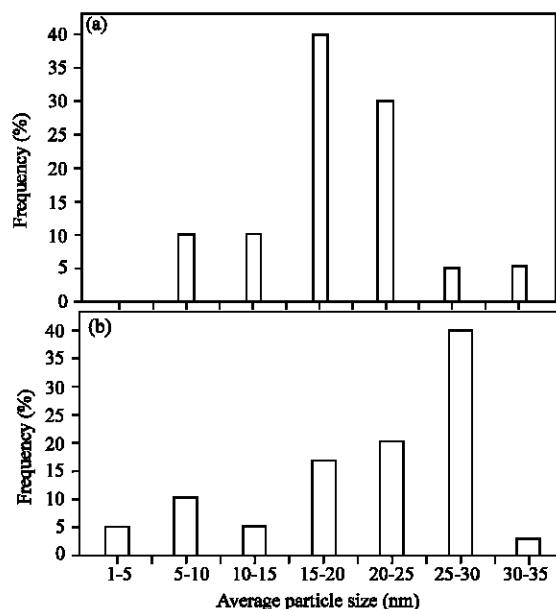


Fig. 6: TEM plots of the catalysts (a) 5% CoMo (50:50)/Alumina and (b) 10% CoMo (50:50)/Alumina

Table 1: Textural properties

No.	Species	BET Surface area (m <sup>2</sup> g <sup>-1</sup> )	Total pore volume (cm <sup>3</sup> g <sup>-1</sup> )	Average pore diameter (nm)
<b>5% M/Alumina</b>				
1	Alumina	190	0.1	9.8
2	5%C	180	0.267	7.5
3	5%Mo	130	0.2	6.9
4	5%CoMo (50:50)	107	0.221	8.2
<b>10% M/Alumina</b>				
1	10%Co	100.6225	0.242119	8.1
2	10%M	107.6394	0.229316	7.9
3	10%CoMo (50:50)	100.1427	0.223671	7.8

**N<sub>2</sub>-adsorption:** Table 1 shows the BET surface area analysis of the catalysts. It was found that surface area of the 5% Co/Alumina and 5% Mo/Alumina was reduced by 5 and 31%, respectively, similarly pore volume and pore size of these catalyst samples were found to be less than the alumina, this could possibly be due to the blockage of the pores of the support with the metal particles. Greater reduction in the surface area of the bimetallic 5% CoMo/Alumina (43%) could be attributed due to the bigger metal particle size. Reduction in the surface area, pore volume and pore size was more pronounced for the catalysts with the increase in loading from 5 to 10 wt.%. For the 10% Co/Alumina surface area was reduced by 47% and for 10% Mo/Alumina it was found to be reduced by 43% while for the bimetallic 10%

CoMo/Alumina the reduction was 45%. Pronounced reduction in the surface area for the catalysts with 10 wt.% metal loading could possibly be due to the blockage of the pore with the metal particles which are bigger in size than the catalysts with 5 wt.% metals loading.

## CONCLUSIONS

It was found that incorporation of Mo (up to 50 wt.%) to the cobalt nano-catalysts increases the reduction temperature by approximately 44% but the percentage of species reducing at lower temperature increased with further increase in the amount of (up to 70 wt.%) Mo. TEM analysis revealed that bimetallic nano-catalyst resulted in better dispersion and decrease in the metal particle size. Surface area and pore volume were found to be lower for all the catalysts than the support, possibly due to the blockage of the support pores by the metal particles, this behavior was more pronounced for the bimetallic nano-catalysts.

## ACKNOWLEDGMENT

The author acknowledges financial support provided by MOSTI (E-Science fund (project No. 03-02-02-SF0036).

## REFERENCES

- Berge, P.J., V.J.V.D. Loosdrecht and A.M.V.D. Kraan, 2000. Oxidation of cobalt based fischer-tropsch catalysts as a deactivation mechanism. *Catal. Today*, 58: 321-334.
- Brady, R.C. and R. Pettit, 1980. Reactions of diazomethane on transition-metal surfaces and their relationship to the mechanism of the Fischer-Tropsch reaction. *J. Am. Chem. Soc.*, 102: 6181-6182.
- Chen, S. and X. Liu, 1991. Efficiency evaluation of combined intervention measures with improving drinking water first to prevent infantile acute diarrhea. *Zhonghua Liu Xing Bing Xue Za Zhi*, 12: 289-291.
- Chen, H. and A.A. Adesina, 1994. Improved alkene selectivity in carbon monoxide hydrogenation over silica supported cobalt-molybdenum catalyst. *Applied Catal. A: General*, 112: 87-103.
- Cooper, C.G., T.H. Nguyen, Y.J. Lee, K.M. Hardiman, T. Safinski, F.P. Lucien and A.A. Adesina, 2007. Alumina-supported cobalt-molybdenum catalyst for slurry phase fischer-tropsch synthesis. *Catal. Today*, 131: 255-261.
- Dry, M.E., 1999. Fischer-tropsch reactions and the environment. *Applied Catal. A: General*, 189: 185-190.

- Iglesia, E., 1997. Design, synthesis and use of cobalt-based fischer-tropsch synthesis catalysts. *Applied Catal. A: General*, 161: 59-78.
- Jacobs, G., T.K. Das, Y. Zhang, J. Li and B.H. Davis, 2002. Fischer-tropsch synthesis: Support, loading and promoter effects on the reducibility of cobalt catalysts. *Applied Catal. A: General*, 233: 263-281.
- Jacobs, G., J.A. Chaney, P.M. Patterson, T.K. Das and B.H. Davis, 2004. Fischer-Tropsch synthesis: Study of the promotion of Re on the reduction property of Co/Al<sub>2</sub>O<sub>3</sub> catalysts by in situ EXAFS/XANES of Co K and Re LIII edges and XPS. *Applied Catal. A: General*, 264: 203-212.
- Khodakov, A.Y., W. Chu and P. Fongarland, 2007. Advances in the development of novel cobalt fischer-tropsch catalysts for synthesis of long-chain hydrocarbons and clean fuels. *Chem. Rev.*, 5: 1692-1744.
- Rodriguez, J.A., S. Chaturvedi, J.C. Hanson and J.L. Brito, 1999. Reaction of H<sub>2</sub> and H<sub>2</sub>S with CoMoO<sub>4</sub> and NiMoO<sub>4</sub>: TPR, XANES, time-resolved XRD and molecular-orbital studies. *J. Phys. Chem. B*, 103: 770-781.
- Sundaramurthy, I., V. Eswaramoorthi, N. Das, A.K. Dalai and J. Adjaye, 2008. Application of multi-walled carbon nanotubes as efficient support to NiMo hydrotreating catalyst. *Applied Catal. A*, 339: 187-195.
- Tavasoli, A., Y. Mortazavi, A. Khodadadi and K. Sadagiani, 2005. Effects of different loadings of Ru and Re on physico-chemical properties and performance of 15% Co/Al<sub>2</sub>O<sub>3</sub> FTS catalysts. *Iran. J. Chem. Chem. Eng.*, 24: 9-17.